GA–A22250

STUDY OF THE CONDITIONS FOR SPONTANEOUS H–MODE TRANSITIONS IN DIII–D

by
T.N. CARLSTROM and R.J. GROEBNER

JANUARY 1996

GENERAL ATOMICS

DISCLAIMER

GA–A22250

STUDY OF THE CONDITIONS FOR SPONTANEOUS H–MODE TRANSITIONS IN DIII–D

by
T.N. CARLSTROM and R.J. GROEBNER

This is a preprint of an invited paper to be presented at the Thirty-Seventh American Physical Society Annual Meeting, Division of Plasma Physics, November 6–10, 1995, Louisville, Kentucky and to be published in *Phys. Plasmas.*

Work supported by
the U.S. Department of Energy
under Contract No. DE-AC03-89ER51114

GA PROJECT 3466
JANUARY 1996

ABSTRACT

A series of scaling studies attempting to correlate the H(high)–mode power threshold (P_{TH}) with global parameters have been conducted. Data from these discharges is also being used to look for dependence of P_{TH} on local edge parameters and to test theories of the transition. Boronization and better operational techniques have resulted in lower power thresholds and weaker density scaling. Neon impurity injection experiments show that radiation also plays a role in determining P_{TH}. A low density threshold for the L(low)-H(high) transition has been linked with the locked mode low density limit, and can be reduced with the use of an error field correcting coil. Highly developed edge diagnostics, with spatial resolution as low as 5 mm, are used to evaluate how the power threshold depends on local edge conditions. Preliminary analysis of local edge conditions for parameter scans of n_e, B_T, and I_p in single-null discharges, and the X-point imbalance in double-null discharges show that, just before the transition to H–mode, the edge temperatures near the separatrix are approximately constant at $100 < T_i < 220$ eV and $35 < T_e < 130$ eV, even though the threshold power varied from 1.5 to 14 MW. During a density scan, the edge ion collisionality, ν_{*i}, varied from 2 to 17, demonstrating that a transition condition as simple as ν_{*i} = constant is inconsistent with the data. The local edge parameters of n_e, T_e, and T_i do not always follow the same global scaling as P_{TH}. Therefore, theories of the L-H transition need not be constrained by these scalings.

I. INTRODUCTION

Studying the conditions necessary for spontaneous H(high)–mode transitions is important both for predicting the operational regime of future devices such as the International Thermonuclear Experimental Reactor[1] (ITER) and for understanding the physics of this important confinement regime. Recent scaling projections[2] indicate that the H–mode power threshold may dominate the auxiliary power requirements for ITER and the conditions needed to obtain H–mode may severely limit the operational space in which ITER may access ignition.[3] It is therefore important to understand the necessary conditions for obtaining H–mode and, in a broader view, to understand the physics of the transition itself.

Although nature has been generous in providing a regime of enhanced confinement that spontaneously develops in these plasmas, she has been reluctant to reveal how the process occurs. At present, the existence of a key parameter associated with the L(low)-H(high) transition has not been experimentally demonstrated. The pulse of power associated with a sawtooth crash that reaches the edge of the plasma or an increase in auxiliary heating power are two ways in which spontaneous transitions can be induced. However, in both cases a trigger or precursor of the L to H transition has remained undetected. Several groups have reported that the edge temperature, or something related to it, is important for the L-H transition. However, the value of the critical edge temperature differs in various devices and it may have other dependencies associated with it.

The model of **ExB** shear flow stabilization of turbulence has provided a semi-quantitative understanding of the confinement improvement that occurs after the L to H transition.[4]

Experimental measurements of the edge radial electric field shear and poloidal rotation have supported and encouraged theoretical work in this area.[5]

For an understanding of the L-H transition, the question now becomes, how does E_r form and what triggers the formation? Several possible mechanisms have been suggested by theory. The loss of epithermal trapped particles scattering into the loss cone at the plasma edge when $\nu_{*i} < 1$ has been proposed by Shaing and Crume.[6] Edge gradients reaching a critical value are included in theories by Itoh and Itoh,[7] by Hinton and Staebler[8] and Cordey *et al.*[9] The formation of E_r arising from the turbulent Reynolds stress has been proposed by Diamond and Kim.[10] E_r caused by the radial gradient of the poloidally asymmetric portion of the radial particle flux has been proposed by Hassam *et al.*[11]

In contrast to understanding of the improved confinement in H–mode, experimental verification and testing of theories of the L-H transition have made much slower progress. This has been partly due to the lack of measurements of important quantities such as turbulent spectra, correlation lengths, and the Reynolds stress tensor in the L–mode edge region prior to and at the L-H transition. It is also due to the lack of guidance from experiment. With available diagnostics, very little is observed to evolve in the edge region in a systematic way prior to the transition.

Because of the complex connection between global parameters and the local parameters in the region where the transition first appears, a satisfactory understanding of the conditions for spontaneous H–mode and comparison to theories can only be made through a detailed analysis of edge parameters. Several theories discuss effects which occur on scale lengths on the order of the poloidal gyroradius, which is typically about 1 cm in present day machines. Therefore, high spatial edge resolution is required to observe "local" edge parameters. The highly developed edge diagnostics on DIII–D,[12] with spatial resolution as low as 5 mm, are well suited to evaluate how the power threshold depends on local edge conditions.

In this paper we report on the global scaling results of a density scan in which the high end of the density range was influenced by radiation, and the low density range was influenced by locked modes. A minimum in the power threshold was observed at moderate densities. Neon impurity injection experiments show that radiation losses inside the separatrix play a role in determining the power threshold. Finally, preliminary analysis of local edge conditions for parameter scans of $\bar{n}_e$, B_T, and I_p in single-null discharges, and the X-point imbalance in double-null discharges are reported.

II. GLOBAL SCALING

Global scaling studies in DIII–D have previously found that the H–mode power threshold increases with the line density, $\bar{n}_e$, the toroidal field, B_T, and is relatively insensitive to the plasma current, I_p.[13] This result was surprising since energy confinement had just the opposite scaling with these parameters. Comparisons of many different machines also indicate an $\bar{n}_e B_T$ scaling if the power is normalized to the plasma surface area, S, suggesting that power flow through the edge region is an important parameter.[2] When the ∇B drift direction is toward the X-point location the power threshold is reduced by about a factor of two. Counter neutral beam injection on DIII–D has about a 10% lower power threshold than for co-injection. There exist other factors which are less well quantified. Boronization and better operational techniques have resulted in lower power thresholds and weaker $\bar{n}_e$ scaling.[14]

These evolving dependencies have led us to re-examine the density dependence of the power threshold with particular attention to the high and low density limits. A plot of the total input power needed to obtain H–mode for a density scan, shown in Fig. 1(a), shows that higher powers are required at high and low density but that a minimum power exists at moderate densities. In this scan, the plasma current and toroidal field were fixed while the target density was varied from shot to shot. The power threshold was measured by increasing the duty cycle of a 50 Hz modulated neutral beam in 300 ms steps. For this study, the minimum beam power step was 0.3 MW. (Further details of this procedure can be found in Ref. 14.) The lowest density point occurred just above the locked mode limit in DIII–D. The higher power at this low density was probably due to the requirement of a neutral beam during the initial current ramp phase of the

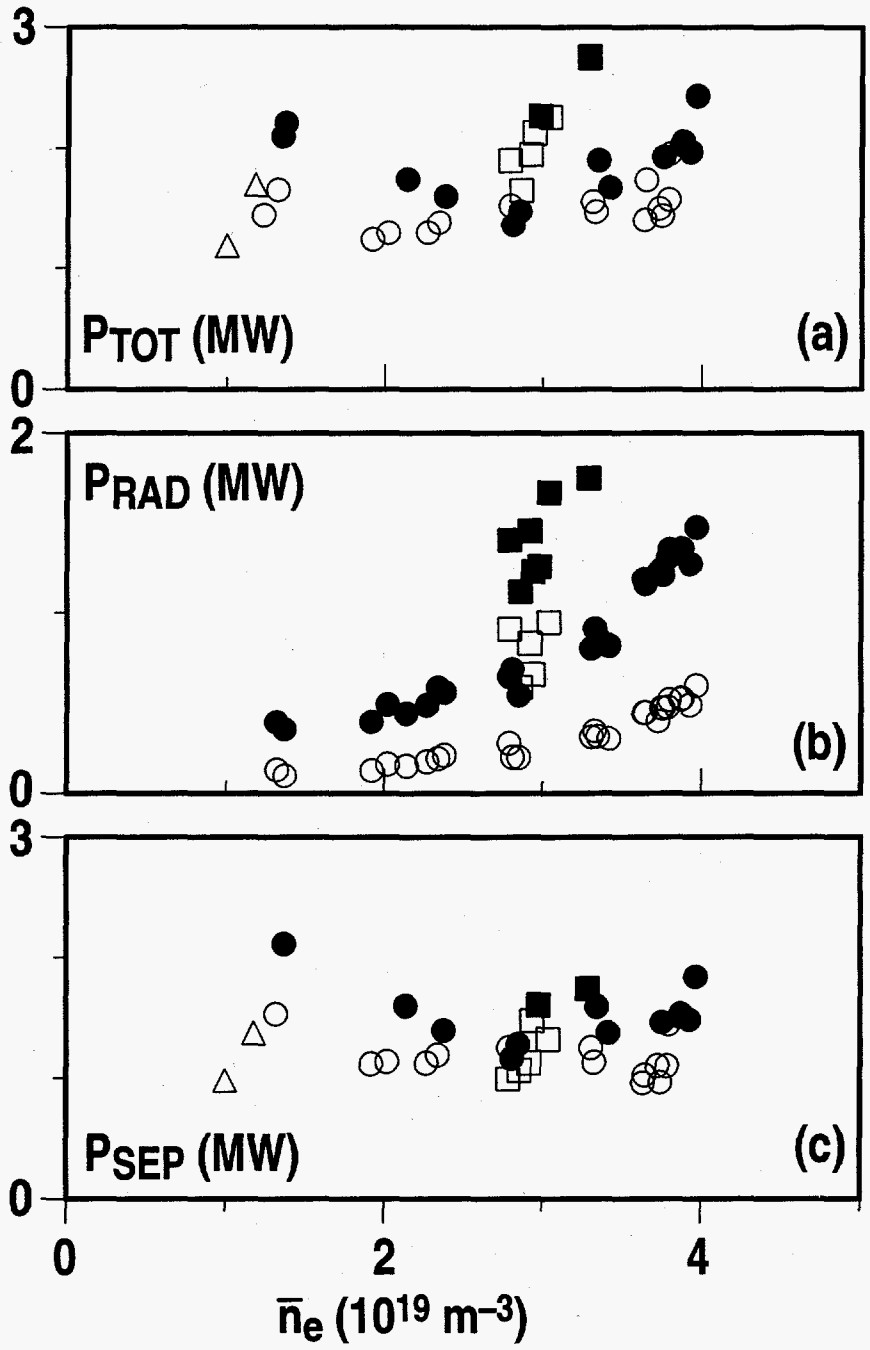

FIG. 1. (a) Total input power, P_{TOT}; (b) radiated power, P_{RAD}; and (c) power flow through the separatrix, P_{SEP}, as a function of the line average density, $\bar{n}_e$, taken from a shot-to-shot scan of the target density. For (a) and (c) the solid points obtain H–mode, the open points remain L–mode, the squares are with neon injection, the triangles are with the C-coil. For (b) the solid points are P_{RAD}(TOT), the open points P_{RAD}(CORE). Discharges used for this survey were lower single-null with the ion ∇B drift direction toward the X-point, I_P = 1.35 MA and B_T = 2.1 T.

discharge to avoid locked modes. When a field error correcting coil[15] was used to reduce the locked mode density limit, the increase of the power threshold at low density was essentially eliminated.

The high density value of this scan was limited by thermal condensation effects,[16] which are also known as multifaceted asymmetric radiation from the edge[17] (Marfe). To achieve target densities above 4×10^{19} m^{-3}, excessive neutral pressures [as shown in Fig. 2(a)] were required. These attempts resulted in Marfe formations which inhibit the L-H transition. Increasing the input power eliminates the Marfe and an L-H transition usually immediately follows. These discharges were not included in this power survey because the power level at the transition represents the level needed to eliminate the Marfe and does not represent the intrinsic L-H power threshold.

Figure 1(a) also shows the increase in power required when a small puff of neon is introduced into the plasma in order to simulate impurities from poorly conditioned walls. Two discharges with neon puffing are indicated. Figure 1(b) shows the total and core radiation losses for these discharges. The radiation profiles are determined from an inversion of a 48-channel bolometer array,[18] with an estimated error of 10–20%. As can be seen from the figure, the addition of the neon impurity can significantly increase the radiation losses and the power threshold.

There is considerable evidence to suggest that the transition takes place at the edge of the plasma and therefore, it is the power flow through the edge that is important. With this insight, we may more accurately determine the relevant power by defining the power across the separatrix as: $P_{SEP} = P_{Ohm} + P_{abs} - dW_p/dt - P_{rad}(core)$; where P_{SEP} is the power across the separatrix, P_{Ohm} is the ohmic input power given by: $P_{Ohm} = V_{surf} \times I_p - dW_b/dt$; V_{surf} is the surface voltage, I_p is the plasma current, dW_b/dt is the time rate of change of the magnetic energy, dW_p/dt is the time rate of change of the plasma energy, and $P_{rad}(core)$ is the radiation

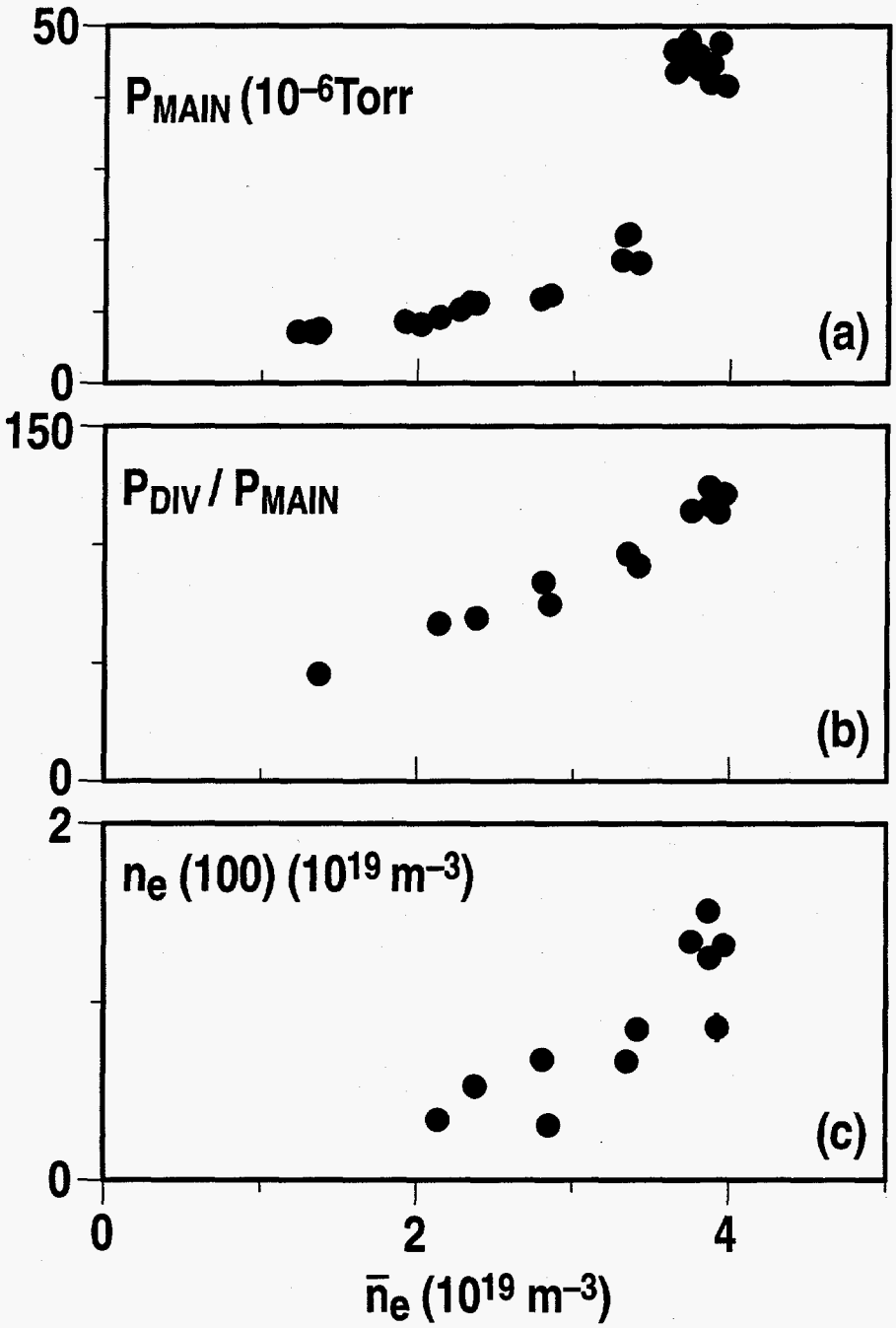

FIG. 2. (a) Neutral pressure measured near the vessel midplane as a function of line average density; (b) compression ratio between the divertor and midplane neutral pressures ; and (c) edge n_e at the separatrix measured by Thomson scattering as a function of line average density taken during the density scan of Fig. 1. Error bars representing 1 σ statistical uncertainties associated with the Thomson scattering measurements are typically smaller than the size of the symbol.

loss from within the separatrix. P_{abs} is the absorbed heating power where we have used the injected neutral beam power corrected for shinethrough losses. The fast ion orbit and charge exchange losses are estimated to be small, <10%.

When it is defined as P_{SEP}, the power threshold has a very weak density dependence, as shown in Fig. 1(c). There is still a slight minimum at moderate density but the increase of power at high density is much reduced. The neon points are now only slightly higher than the others indicating that the radiative losses within the separatrix account for most of the increase of the power threshold with neon puffing.

The effect of neutrals on the L-H transition can be complex. It has been speculated that the penetration of neutrals through the scrape-off layer and into the edge plasma can change the momentum balance, charge exchange losses, and density and pressure gradients. All these effects could have an impact on the physics of the L-H transition. Measurement of the edge neutral density profile is difficult and to our knowledge, no direct measurements relevant to L-H transitions on tokamaks have been reported. However, modeling of the neutral density using the Monte Carlo code, DEGAS, and measured D_α line intensity and scrape-off layer plasma parameters has been done for the JT-60U tokamak.[19] They found that the ν_{i*eff} value at the H-transition tends to decrease with increasing neutral density, suggesting that the neutrals have a substantial influence on the edge conditions at the H-transition.

In lieu of direct neutral density measurements, Fig. 2(a) shows the neutral pressure measured near the midplane for the density scan previously discussed. The pressure increases non-linearly with the line average density. This implies a decrease in the fueling efficiency probably owing to a decrease in the neutral mean-free-path as the scrape-off density increases. In Fig. 2(b) we show the ratio of the neutral pressure below a baffle plate in the divertor region to the midplane pressure. This compression ratio is nearly a linear function of the density, indicating that the

divertor is more effective at confining neutrals as the density is increased. This can be understood from the mean-free-path arguments just discussed. Figure 2(c) shows n_e at the separatrix, measured by Thomson scattering, increasing roughly linearly with the line average density . The behavior of the edge n_e is similar to, but less pronounced than the neutral pressure. However, the result of the power threshold having only a weak dependence on density suggests that the neutral pressure has very little effect on the conditions for the L-H transition. This is true for only a limited range in pressure and density. For instance, if the gas puff rate is sufficiently high that the plasma detaches or forms a Marfe, the L-H transition can be suppressed.

III. LOCAL EDGE MEASUREMENTS

In order to better understand and interpret the global scaling results, and to improve the quantitative comparisons between theory and experiment, we have measured the electron density, n_e, electron temperature, T_e, and ion temperature, T_i, edge profiles just prior to the L-H transition. Measurements were also made in L–mode and H–mode phases for comparison. The edge profiles of n_e and T_e were measured with a multipoint, multipulse Thomson scattering system.[20] This system has a high density of edge chords, which provides a spatial resolution of 0.75 cm when projected to the vessel midplane. In addition, this system uses eight YAG lasers controlled by a flexible timing system which provided data every 5 to 25 ms. The edge values of T_i were measured with a multipoint Charge Exchange Recombination (CER) system which also has a high density of edge chords, with a spatial resolution capability of 0.3 cm.[21] For most of the data presented here, the spatial resolution is 0.6 cm. This system is designed for fast readout of the detector and has a minimum temporal resolution of 0.5 ms. The data for the CER system were obtained from the C VI 5290 A line excited by charge transfer between one of the heating neutral beams and fully ionized carbon ions in the plasma.

Typical edge profiles in L–mode and H–mode showing rapid variation with radius near the plasma edge are shown in Fig. 3. The Thomson measurements of n_e and T_e are mapped to the midplane using the magnetic equilibrium code EFIT,[22] which typically determines the separatrix position to ±0.5 cm. For our analysis, the data are fit with a smooth spline curve and the values at normalized toroidal flux, $\rho = 0.90, 0.95, 0.98$, and 1.00 are recorded in a database.

The H–mode transport barrier forms just inside the separatrix and this is the edge region we are studying to determine local conditions for the L-H transition. Figure 4 shows $T_e(90)$, $T_e(95)$

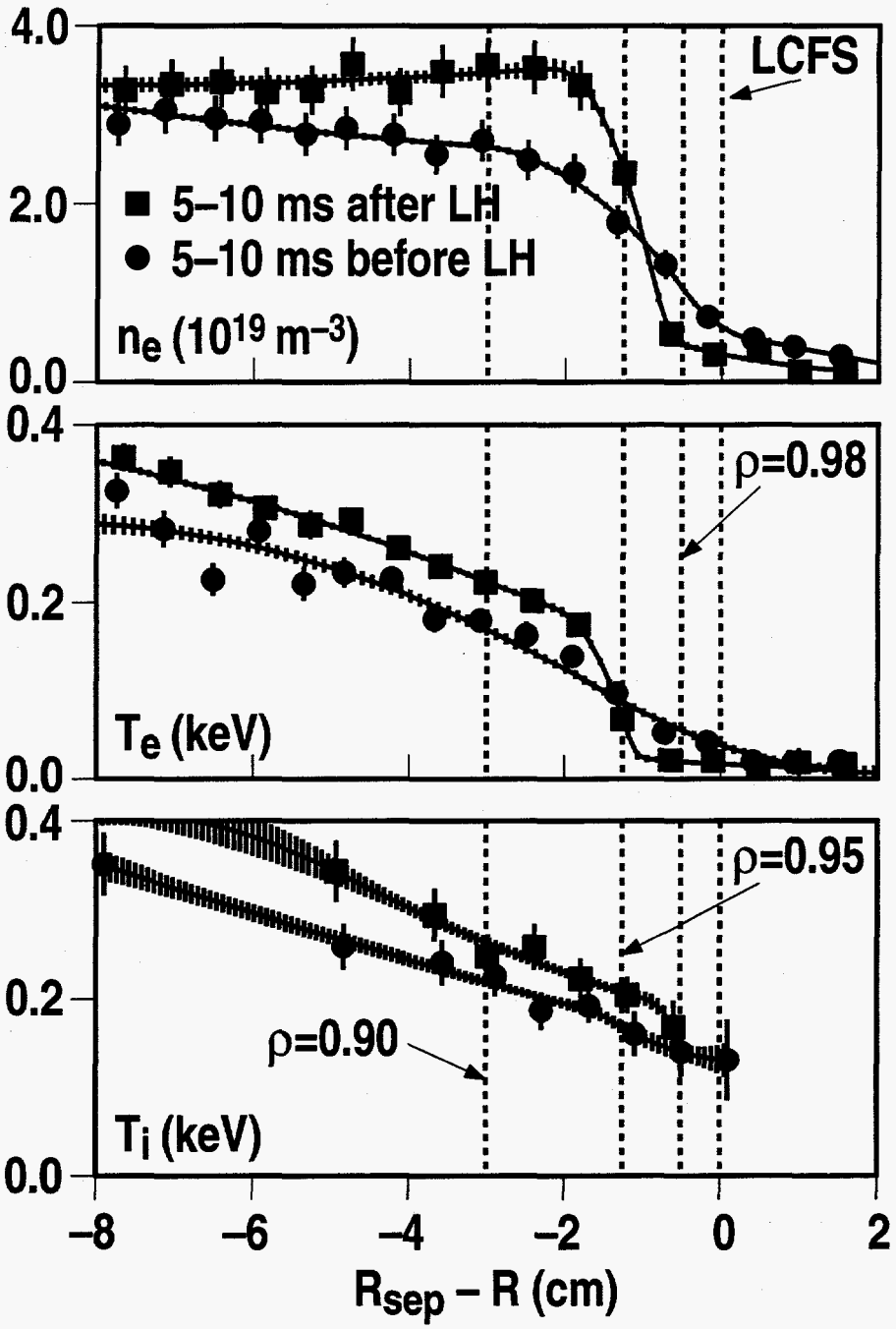

FIG. 3. Radial edge profiles of n_e, T_e, and T_i, measured with Thomson scattering and CER, just before and after an L-H transition. Discharge conditions were I_P = 1.35 MA, B_T =2.1 T, P_{TOT} = 2.0 MW, $\overline{n}_e = 4.0 \times 10^{-19}$ m^{-3}.

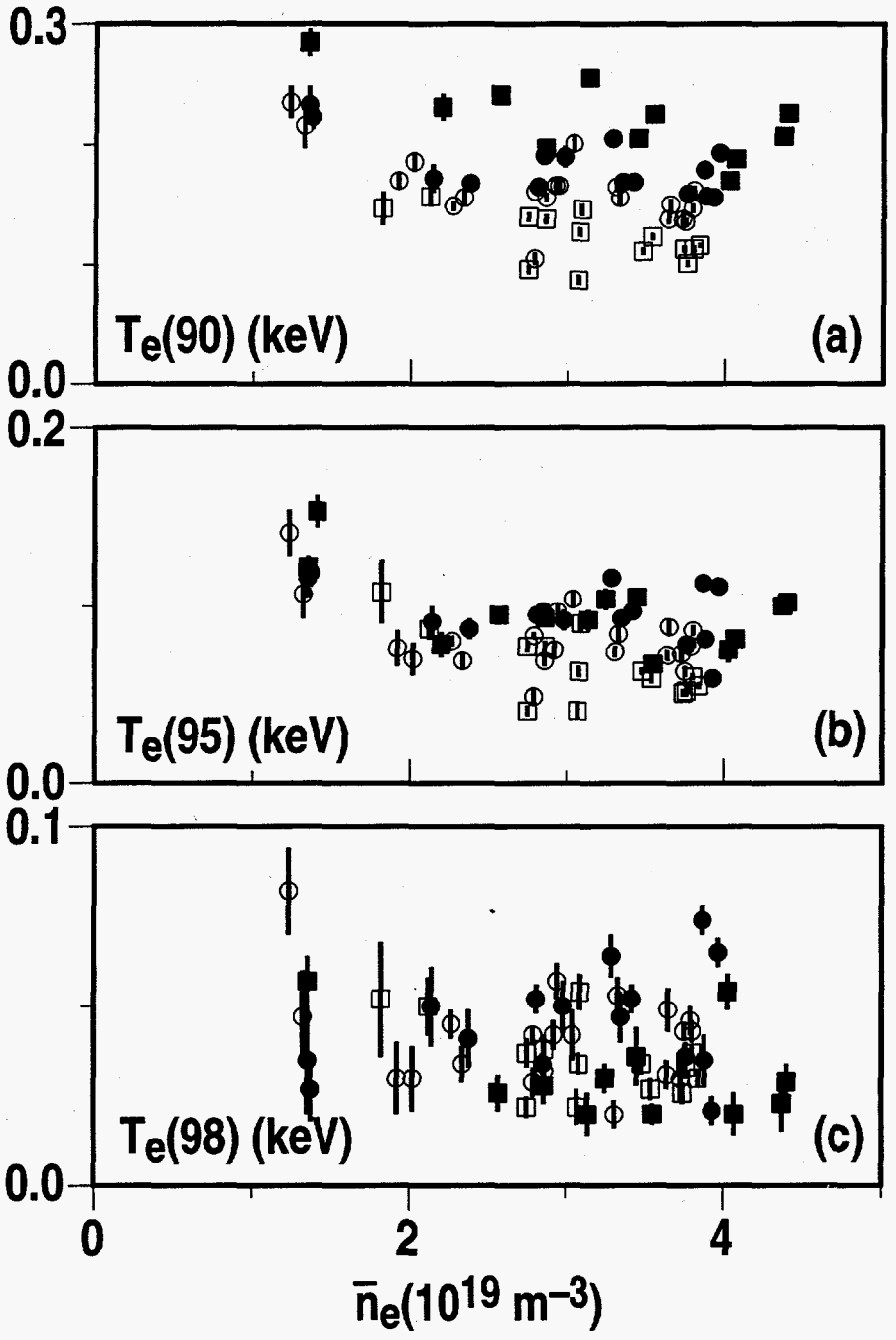

FIG. 4. Edge T_e at ρ = 0.90, 0.95, and 0.98 for the density scan of Fig. 1. The solid squares are just after the L-H transition, the solid circles are just before the transition, the open circles are L–mode, and the open squares are Ohmic. The error bars represent the 1 σ statistical uncertainties associated with the Thomson scattering measurement.

and $T_e(98)$, evaluated at $\rho = 0.90$, $\rho = 0.95$ and $\rho = 0.98$ respectively, during L–mode, just before (5–10 ms) the L-H transition (pretransition), and just after (5–10 ms) the L-H transition (H–mode) for the density scan. At $\rho = 0.90$ there is a clear separation between the Ohmic points and the L–mode points, indicating the effect of auxiliary heating. However, there is little distinction between the L–mode and pretransition points, which indicates that additional heating power has only a weak effect on T_e. The H–mode points are higher than the pretransition points indicating this location is inside the H-mode transport barrier. Within the scatter of the data, there is almost no dependence of T_e on the line average density. At $\rho = 0.95$, the situation is different, with the L–mode, pretransition, and H–mode points all clustering together. This indicates that this location is near the pivot point as the radial profiles change from L–mode to H–mode. At $\rho = 0.98$, the H–mode points generally fall below the L–mode and pretransition points, indicating that this location is outside the transport barrier. Because the transport barrier appears to form at around $\rho = 0.95$, we will concentrate our analysis at that location.

Local edge parameters evaluated at $\rho = 0.95$ for the density scan are shown in Fig. 5 for L–mode, pretransition, and just after the H–mode phase of the discharge. We are expecting a parameter important for the L-H transition to evolve to a critical value just prior to the transition. Although significant scatter in the data exists, there is a general trend that T_e and T_i increase going from ohmic to L–mode to H–mode and that the pretransition points are relatively constant, independent of $\bar{n}_e$. This result supports previous findings that the edge temperatures may be related to the critical parameter for the L-H transition. The variation of the edge density suggests that it is not related to the critical parameter.

The lack of clear distinction between L–mode, pretransition, and H–mode points for n_e, T_e, and T_i makes it difficult to quantify the importance of the evolution of these parameters for the L-H transition. Figure 6 shows the edge temperatures and electron pressure as a function of P_{SEP}. The weak dependence of these parameters on P_{SEP} may indicate that there is too much

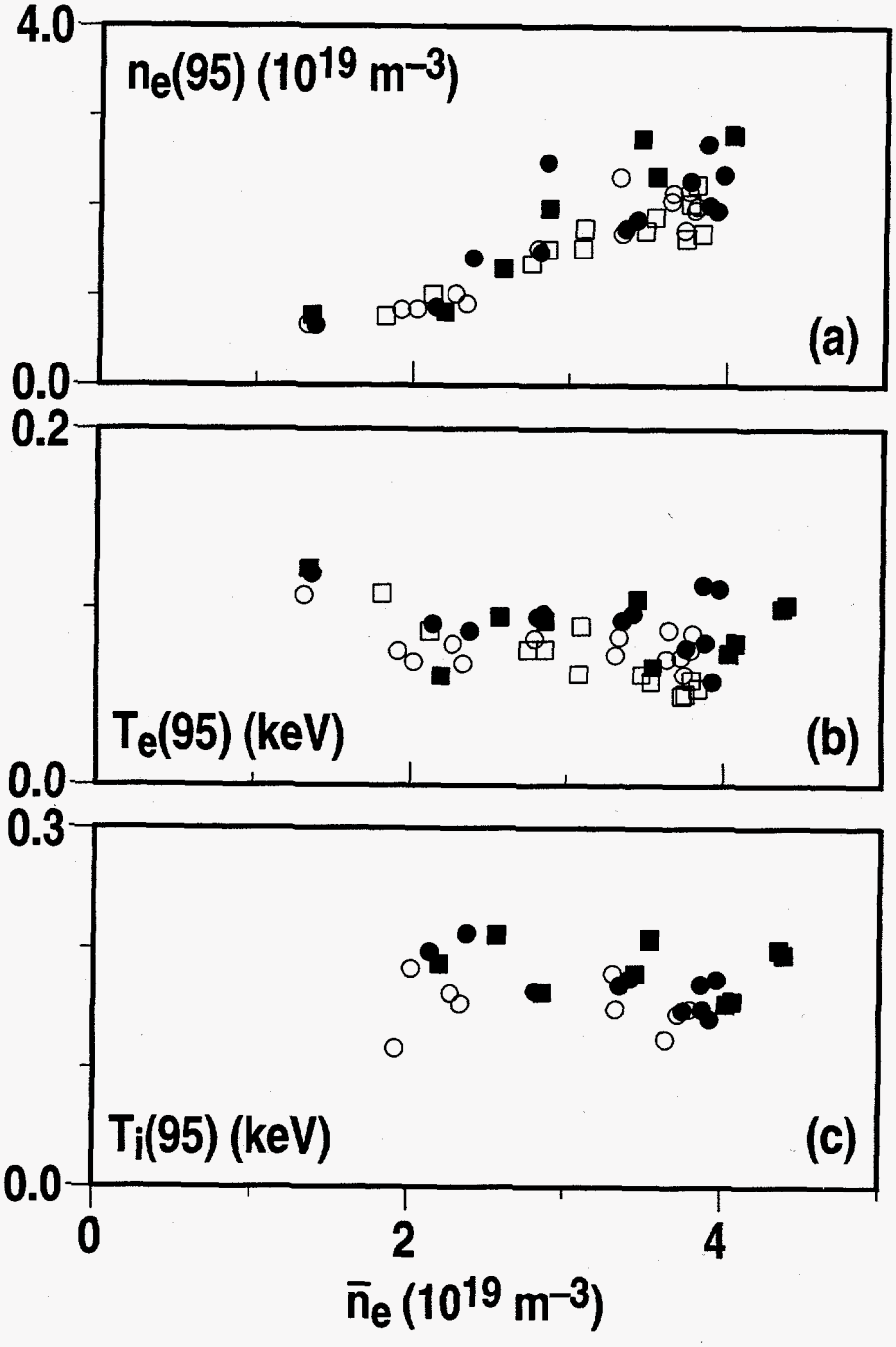

FIG. 5. Edge parameters of n_e, T_e, and T_i, evaluated at $\rho = 0.95$, for the density scan. The solid squares are just after the L-H transition, the solid circles are just before the transition, the open circles are L–mode, and the open squares are *Ohmic*.

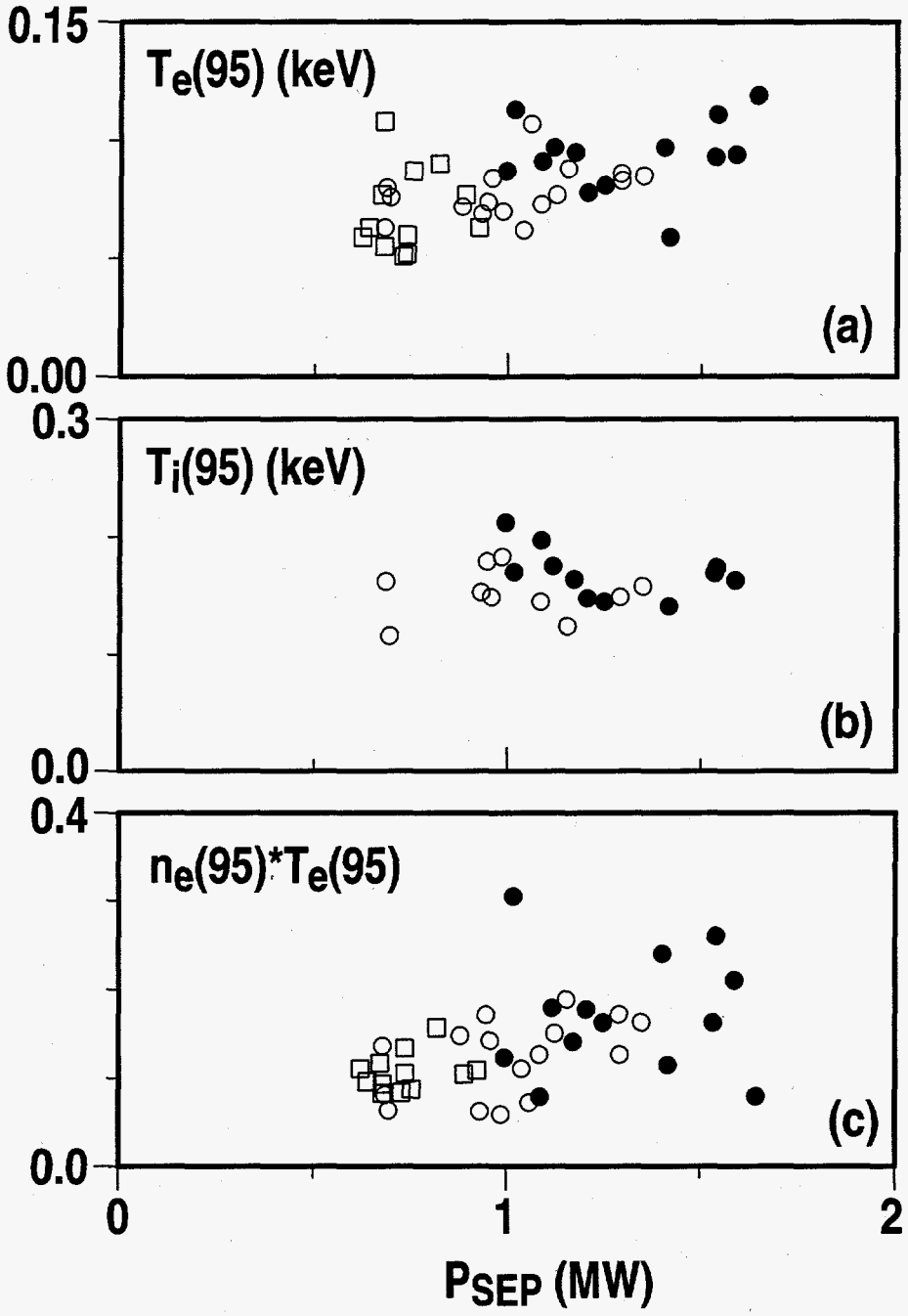

FIG. 6. Edge parameters of T_e, T_i, and n_eT_e at $\rho = 0.95$ as a function of P_{SEP} for the density scan. The solid circles are just before the transition, the open circles are L–mode, and the open squares are Ohmic.

scatter in our data to resolve the small changes of these quantities, or it may suggest that the radial gradients of these parameters are more important for the transition. Figure 7 shows the normalized radial gradients of these edge parameters. The density gradients scatter between 0.2 and 0.6 cm^{-1} for Ohmic, L–mode, and pretransition points with the H–mode points generally at higher values. There is no particular $\bar{n}_e$ dependence. There is some progression of the density gradient increasing from Ohmic to L–mode to pretransition at low to mid $\bar{n}_e$, but no progression is observed at high $\bar{n}_e$. The T_e gradients scatter between 0.4 and 1.2 cm^{-1} with no apparent dependence on $\bar{n}_e$ or progression from Ohmic to H–mode. The T_i gradients are about half of the T_e gradients, and show a similar lack of dependence on $\bar{n}_e$ or discharge mode. Because of the large scatter and lack of a clear distinction between modes, we cannot draw any significant conclusions regarding the importance of the edge gradients to the L-H transition at this time.

Figure 8 shows several quantities calculated from the previous data. The ion collisionality is calculated using the definition given by Kim[23] for arbitrary shape and aspect ratio, and substituting n_e for n_i (assumes $Z_{eff} = 1$). It shows an almost linear dependence on the line average density. This result indicates that the threshold condition is not as simple as achieving some value of edge ν_{i*}, such as $\nu_{i*} = 1$. The only way to avoid this conclusion is to postulate that the edge n_i actually varied little during the density scan. This seems unlikely, but direct measurements of n_i or Z_{eff} are not available. The ion gyroradius, $\rho_{\theta i}$, remains relatively constant for this scan. The ion pressure scale length, L_{pi}, (again, substituting ne for ni) does evolve from L–mode to H–mode, but the high pretransition points around a density of 4×10^{19} m^{-3} confuse the grouping between L–mode and pretransition points which would indicate that this parameter is evolving toward a critical value prior to the L-H transition. The dimensionless ratio, $\rho_{\theta i}/L_{pi}$, is about 0.5 in L–mode and reaches values around 1 in H–mode, 5–10 ms after the transition.

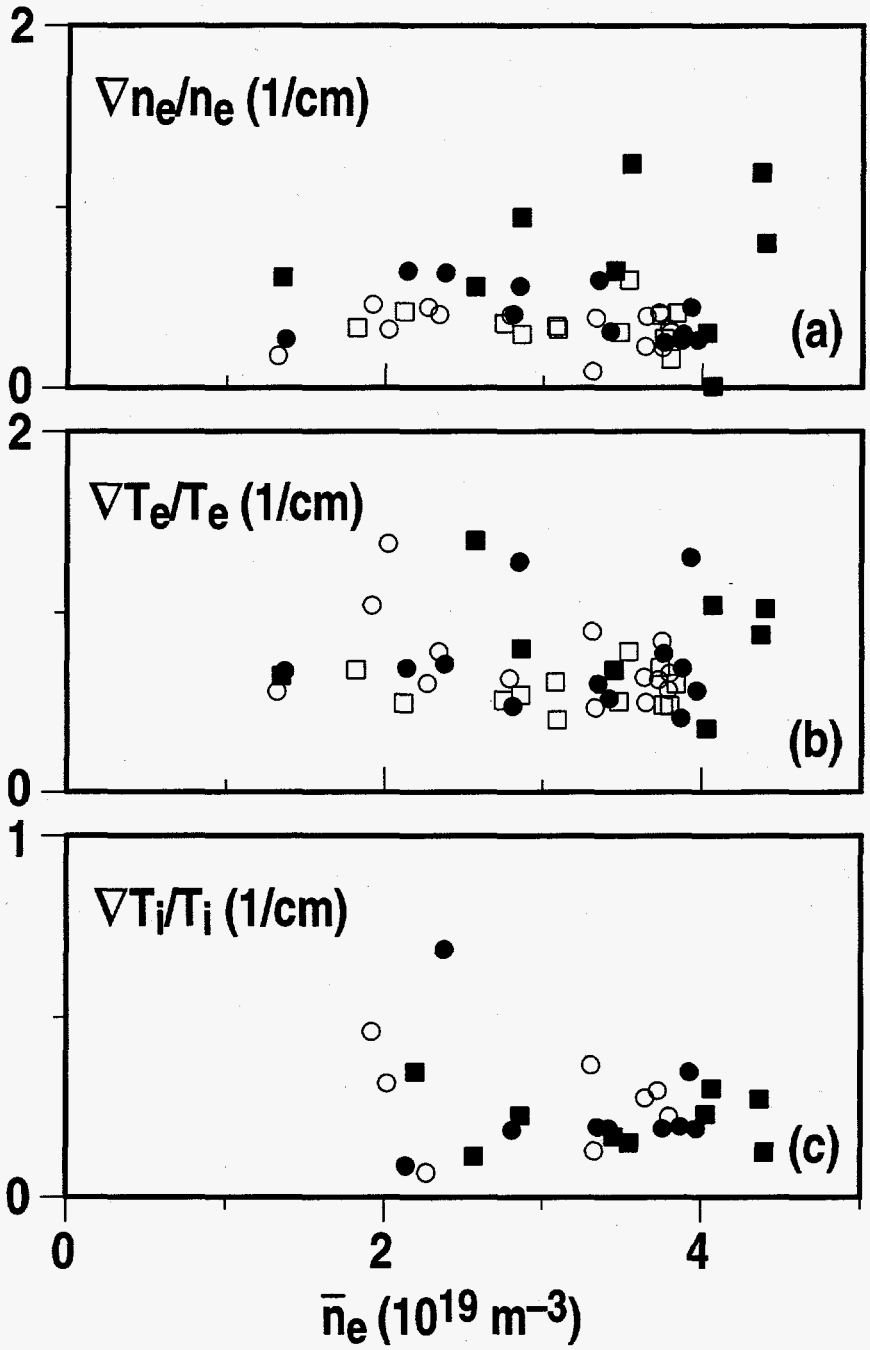

FIG. 7. Edge parameters of $\nabla n_e/n_e$, $\nabla T_e/T_e$, and $\nabla T_i/T_i$, evaluated at $\rho = 0.95$, for the density scan. The solid squares are just after the L-H transition, the solid circles are just before the transition, the open circles are L–mode, and the open squares are Ohmic.

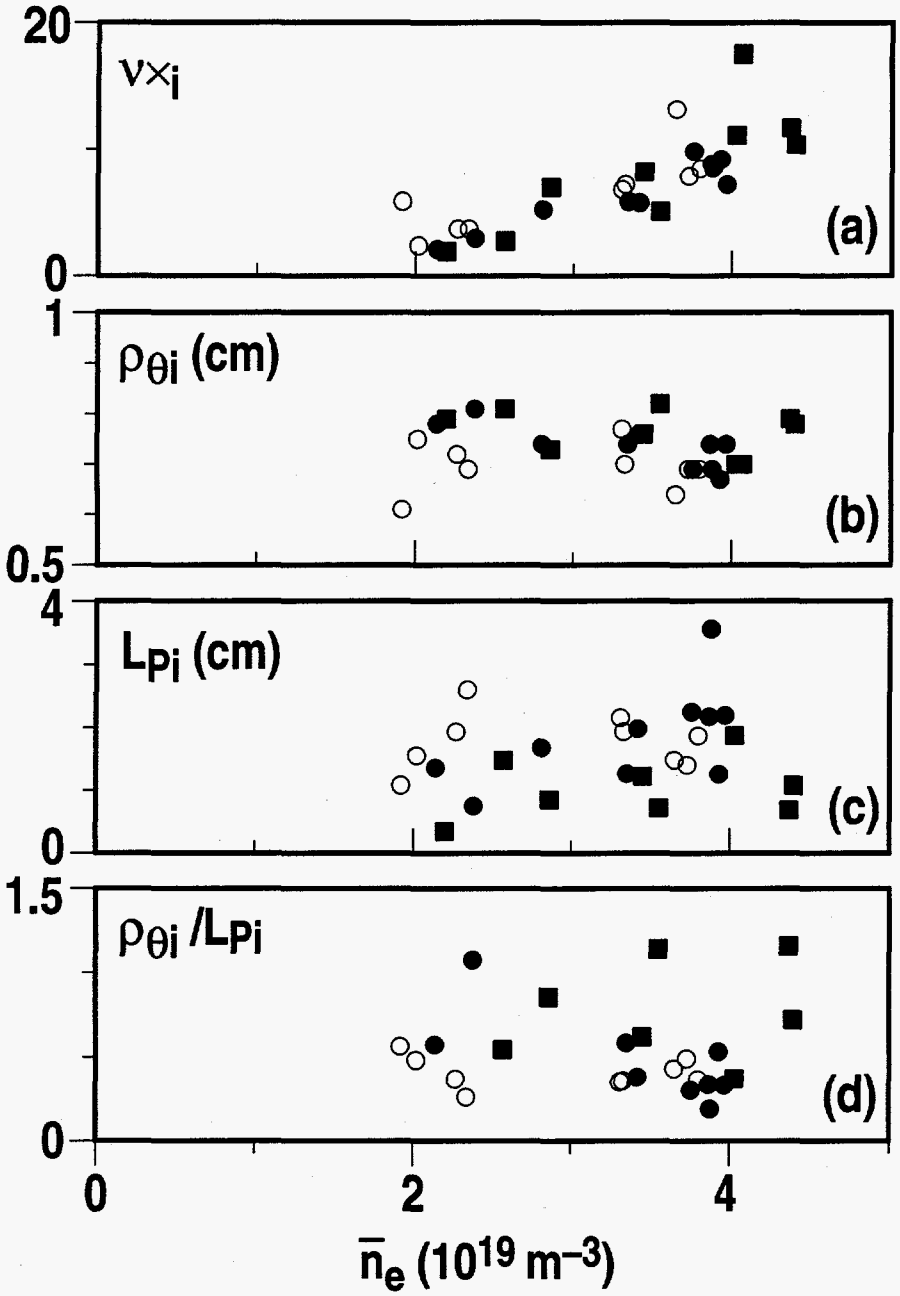

FIG. 8. Edge parameters of ν_{i*}, $\rho_{\theta i}$, L_{Pi}, and $\rho_{\theta i}/L_{Pi}$, evaluated at $\rho = 0.95$, for the density scan. The solid squares are just after the L-H transition, the solid circles are just before the transition, the open circles are L–mode, and the open squares are Ohmic.

Similar analysis was done for pretransition times for the surveys of I_P, B_T, and dr_{sep} reported in Ref. 14. The results are tabulated in Table I. If a parameter varied systematically during a scan, a range is given in the table. If the parameter showed little variation or scattered in a non-systematic way, it is listed as being constant. For the n_e scan previously discussed, $n_e(95)$ and ν_{i*} are listed with ranges, whereas the other pretransition phase parameters are relatively constant.

There is very little change in any of the pretransition edge parameters while B_T was varied from 1.1 to 2.1 T, and the power threshold changed by about a factor of two. Both T_e and T_i are approximately constant but they are roughly 2/3 their corresponding values in the density scan. T_e at $\rho = 0.95$ remained at about 50 eV prior to both the ohmic H–modes at $B_T = 1.1$ T, and the neutral beam H–modes at $B_T = 2.1$ T. ν_{i*} remains high at about 12 but $\rho_{\theta i}$ and L_{pi} are similar to their values in the density scan.

In a previous study of the L-H transition, it was found that the edge T_e measured at $\rho = 0.90$ increased linearly with B_T just before the transition with a proportionality constant of 115 eV/tesla.[13] We find that the edge T_i at $\rho = 0.90$ increases with B_T, but the increase is weaker than linear. The increase at $\rho = 0.95$ is much weaker. In contrast to our previous results, the edge T_e remains nearly constant at both radii. Therefore, the explanation that P_{th} scales with B_T because higher edge temperatures are required at higher B_T only holds if we consider the ion temperature. Our earlier results were obtained prior to boronization of the DIII–D vessel and for hydrogen neutral beam heating of deuterium plasmas. The power threshold was two times higher for those data. The different behavior of T_e and T_i suggests that the i-e energy exchange rate may be important in determining the temperature behavior at the transition. The pretransition T_i points in Fig. 5 show a slight decrease with increasing $\bar{n}_e$, which may be evidence for a stronger coupling to the lower temperature electrons at high density.

Table I. Edge parameters at $\rho = 0.95$ measured just before the L-H transition for various survey scans. A range is given if the parameter varied systematically during a scan.

Survey Scan	$\bar{n}_e$ (10^{19} m^{-3})	I_P (MA)	B_T (T)	dr_{sep} (cm)
Range	1.2 to 4.0	1 to 2	1.1 to 2.1	–0.7 to 0.7
Held fixed				
I_p (MA)	1.35		1.0	1.35
B_T (T)	2.1	2.1	–	2.1
$\bar{n}_e$ (10^{19} m^{-3})	–	4.0	4.0	4.0
P_{tot} (MW)	1.5 to 2.5	2.0 to 2.5	1.0 to 2.0	4.0 to 14
n_e (95) (10^{19} m^{-3})	0.5 to 2.0	2.0 to 4.0	2.0	2.0 to 4.0
T_e (95) (keV)	0.09	0.05 to 0.10	0.05	0.05 to 0.1
T_i (95) (keV)	0.18	0.18	0.10	0.15 to 0.2
$\rho_{\theta i}$ (cm)	0.8	0.8 to 0.5	0.8	0.7
L_{Pi} (cm)	1.6	3.5 to 2.5	2.0	1.0 to 4.0
ν_{i*}	2 to 12	12 to 5	12	10
$\rho_{\theta i}/L_{Pi}$	0.5	0.2	0.4	1.0 to 0.2

Although the threshold power remained nearly constant for the I_P scan, both $n_e(95)$ and $T_e(95)$ increase with I_P. In contrast to the B_T scan, $T_i(95)$ remains nearly constant. Both ν_{i*} and $\rho_{\theta i}$ decrease with increasing I_P. L_{Pi} also decreases with I_P except for the 1 MA case where L_{Pi} is in the range of 1 to 2. The ratio $\rho_{\theta i}/L_{Pi}$ remains relatively constant at about 0.25 for 1.35 and 2.0 MA but at 1.0 MA, it varies between 0.3 and 1.2. The reason for the different behavior of these parameters at the 1 MA level is unknown at this time. Systematic errors in the determination of the separatrix location is one possibility under investigation. This is the only scan where $\rho_{\theta i}$ changes significantly. The fact that, at the higher current levels, L_{Pi} also changes to keep $\rho_{\theta i}/L_{Pi}$ relatively constant suggests that this ratio may be an important parameter for the L-H transition.

The last survey we have examined is a scan of a double-null discharge that was shifted slightly up or down so that the dominant X-point was either towards or away from the ∇B drift direction.[14] When the plasma was balanced ($dr_{sep} = 0$) or shifted down ($dr_{sep} = -0.7$) so that the ∇B drift direction was toward the dominant X-point, the power threshold was about 4 MW. (dr_{sep} is a measure of the distance between the separatrices associated with the two X-points, measured at the plasma midplane.) However, when the plasma was shifted up ($dr_{sep} = 0.7$) and the dominant X-point changed to the top of the vessel, the power threshold increased to over 14 MW. The quantities n_e, T_e, and T_i, all increase with dr_{sep} even though the power at $dr_{sep} = -0.6$ and $dr_{sep} = 0.0$ were about the same. L_{Pi} is a factor of 2 smaller when $dr_{sep} = -0.6$ suggesting the favorable ∇B drift effect may help decrease L_{Pi}. The ratio $\rho_{\theta i}/L_{Pi}$ decreases as dr_{sep} changes from –0.7 to 0.0, even though the power threshold does not change. $\rho_{\theta i}/L_{Pi}$ decreases further at $dr_{sep} = 0.7$ where the power threshold has increased dramatically.

When we compare edge temperatures in H–mode with the pretransition results for the dr_{sep} scan, we find that at $\rho = 0.95$ the H–mode temperatures are lower than the L–mode temperatures. This indicates that $\rho = 0.95$ is outside the transport barrier and suggests a possible problem with our determination of the separatrix location in this configuration. When we evaluate the edge parameters at $\rho = 0.90$, we find that the edge temperatures increase slightly in H–mode, indicating this location is just inside the transport barrier. At this location, $T_e(90)$ and $n_e(90)$ increase slightly when $dr_{sep} = 0.7$, but the remaining parameters, T_i, $\rho_{\theta i}$, ν_{i*}, and L_{Pi}, are relatively constant over the entire dr_{sep} range.

IV. CONCLUSIONS

The density scaling of the H–mode power threshold is due, in part, to the radiation losses from within the separatrix increasing with density. This radiation loss decreases the power flow through the edge region of the plasma and increases the power threshold. Increases in radiation associated with impurities have a similar effect. Thus, for a factor of 3 range of density in DIII–D, the intrinsic n_e scaling of the power threshold is weak or non-existent. An H–mode low density threshold has been linked to the locked mode density limit. The use of an error field correcting coil has reduced the locked mode low density limit and removed the increase of the H–mode power threshold at low density. Locked modes are one of several low density operational constraints that may affect the power threshold. A wide variation of the neutral pressure had little affect on the power threshold.

These results have several implications for obtaining H–mode in future devices, such as ITER. Core radiation losses are important for determining the H–mode power threshold and the scaling of these losses needs to be determined before meaningful power threshold predictions can be made. Machine wall conditions and impurity levels need to be controlled to minimize the power threshold. Operational constraints such as locked mode density limits need to be determined and avoided.

In an attempt to look for dependence of the power threshold on local edge parameters, measurements of n_e, T_e, and T_i at $\rho = 0.95$ have been made just prior to the L-H transition for a wide range of plasma parameters. The edge density at $\rho = 0.95$ varied over a wide range of $0.5 < n_e\ (10^{19}\ m^{-3}) < 4.0$, indicating that the edge n_e is not a critical parameter for the L-H transition. The edge temperatures varied over at range of $0.03 < T_e\ (keV) < 0.13$ and $0.10 < T_i\ (keV) <$

0.22, supporting previous observations from many devices over the last ten years that the edge temperature or something related to it, is important for the L-H transition. The narrow range of T_i compared with T_e suggests that the ions are more important than electrons for the L-H transition. The relatively constant value of T_i in L–mode, pretransition, and just after the transition, in the region where the transport barrier forms, suggests that the edge gradient of T_i, or something related to it, is more important for the L-H transition than just the value of T_i.

According to our criteria, ν_{i*} is not a critical parameter for the transition because it varies over a wide range just prior to the L-H transition. This result is important for L-H theories because it indicates that the threshold condition is not as simple as achieving some value of edge ν_{i*}, such as Shaing's theory[6] which requires $\nu_{i*} = 1$ for ion orbit loss to be important for E_r formation. The large variation of ν_{i*} also suggest that the conditions for the L-H transition are based on a fluid type behavior rather than kinetic effects.

The lack of any systematic changes in the pretransition edge temperatures for a factor of two change in B_T and P_{TH} implies that more power is required to achieve the same edge temperature at higher B_T. For this to be the case, the edge energy confinement would have to decrease with increasing B_T, which seems unlikely. Another interpretation may be that the edge temperatures are held relatively fixed by the strong parallel heat conduction on the nearby open field lines, and the threshold condition is related to energy associated with the power flow across the separatrix. The global scalings previously discussed demonstrate the importance of the power flow across the separatrix. The power flow does not manifest itself through increased gradients, but rather through turbulence. This interpretation supports the theory of Diamond and Kim,[10] in which E_r at the plasma edge arises from the turbulent Reynolds stress tensor. This requires, however, that B_T somehow influences the turbulent formation of E_r.

The effect of the ion ∇B drift direction relative to the X-point location in the d_{rsep} scan had the largest effect on P_{TH}. However, the changes in the edge parameters were modest, especially at $\rho = 0.90$. Again, we are left to conclude that the X-point location has a strong influence on edge confinement or that it influences the formation of E_r.

Unfortunately, the scatter in our edge gradient measurements is too large to make critical assessments of L-H theories that rely on edge gradients. We can say that the edge gradients in L–mode, prior to the transition, are significant with the ratio $\rho_{\theta i}/L_{Pi}$ in the range of 0.5 for most cases. This result supports the theoretical work of Itoh and Itoh,[7] Hinton and Staebler,[8] and Cordey, *et al.*,[9] which rely on gradient scale lengths of a few gyroradii.

Even though P_{TH} may scale with global parameters such as $\bar{n}_e$ and B_T, the local edge parameters of n_e, T_e, and T_i do not always follow the same scaling. Therefore, theories of the L-H transition need not be constrained by the global P_{TH} scalings.

Significant scatter and uncertainties exist in the edge measurements used for this study. Future improvements can be made by comparing edge profile features directly, such as maximum edge gradients, rather than relying on flux surface mapping and determination of the separatrix position, which have uncertainties comparable to the spatial features we are trying to resolve. More shots, especially L–mode, can be analyzed and regression analysis performed to determine the relative importance of various parameters. Further analysis of the main ion radial force balance is required to understand the role of E_r formation and the L-H transition.

STUDY OF THE CONDITIONS FOR SPONTANEOUS H–MODE TRANSITIONS IN DIII–D

T.N. Carlstrom & R.J. Groebner

REFERENCES

[1]K. Tomabechi, Plasma Phys. and Contr. Nucl. Fusion Research 1990 (International Atomic Energy Agency, Vienna, 1991), Vol. 3, p. 217.

[2]F. Ryter, for the H–mode Data Base Working Group, in *Proceedings of the 21st European Physical Society Conference on Controlled Fusion and Plasma Physics,* Montpellier, 1994, (European Physical Society, Petit-Lancy, 1995) Vol. **18B**, p. 334.

[3]D. Boucher and V. Mukhovatov, "Impact of H–mode Power Threshold on ITER Performance and Operation," in *Proceedings of the 5th Workshop on H–Mode Physics*, Princeton, 1995, to be published in Plasma Phys. and Contr. Fusion.

[4]R. J. Groebner, Phys. Fluids B **5**, 2343 (1993).

[5]K. H. Burrell, E. J. Doyle, P. Gohil, R. J. Groebner, J. Kim, R. J. La Haye, L. L. Lao, R. A. Moyer, T. H. Osborne, W. A. Peebles, C. L. Rettig, T. H. Rhodes, and D. M. Thomas, Phys. Plasma **1,** 1536 (1994); R. A. Moyer, K.H. Burrell, T.N. Carlstrom, S. Coda, R. W. Conn, E. J. Doyle, P. Gohil, R. J. Groebner, J. Kim, R. Lehmer, W. A. Peebles, M. Porkolab, C. L. Rettig, T. L. Rhodes, R. P. Seraydarian, R. Stockdale, D. M. Thomas, G. R. Tynan, and J. G. Watkins, Phys. Plasma **2**, 2397 (1995).

[6]K. C. Shaing and E. C. Crume Jr., Phys. Rev. Lett. **63**, 2369 (1989).

[7]S. I. Itoh and K. Itoh, Nucl. Fusion **29**, 1031 (1989).

[8]F. L. Hinton and G. M. Staebler, Phys. Fluids B **5**, 1281 (1993).

[9]J. G. Cordey, W. Kerner, and O. Pogutse, Plasma Phys. and Contr. Fusion, 773 (1995).

[10]P. H. Diamond and Y. B. Kim, Phys. Fluids B **3**, 1626 (1991).

[11]A. B. Hassam, T. M. Antonsen, Jr., J. F. Drake, and C. S. Liu, Phys. Rev. Lett. **66**, 309 (1991)

[12]J. L. Luxon, R. Anderson, F. Batty, C. B. Baxi, G. Bramson, N. H. Brooks, B. Brown, B. Burley, K. H. Burrell, R. Callis, G. Camapbell, T. N. Carlstrom, A. P. Colleraine, J. Cummings, L. Davis, J. C. DeBoo, S. Ejima, R. Evanko, H. Fukumoto, R. Gallix, J. Gilleland, T. Glad, P. Gohil, A. Gootgeld, R. J. Groebner, S.Hanai, J.Haskovec, E. Heckman, M. Heilberger, F. J. Helton, N. Hosogane, C.-L. Hsieh, G. L. Jackson, G. Jahns, G. Janeschitz, E. Johnson, A. G. Kellman, J. S. Kim, J. Kohli, A. Langhorn, L. L. Lao, P. Lee, S. Lightner, J. Lohr, M. A. Mahdavi, M. Mayberry, B. McHarg, T. McKelvey, R. Miller, C.P. Moeller, D. Moore, A. Nerem, P. Noll, T. Ohkawa, N. Ohyabu, T. H. Osborne, D. O. Overskei, P. I. Petersen, T. W. Petrie, J. Phillips, R. Prater, J. Rawls, E. E. Reis, D. Remsen, P. Riedy, P. Rock, K. Schaubel, D. P. Schissel, J. T. Scoville, R. Seraydarian, M. Shimada, T. Shoji, B. Sleaford, J. P. Smith, Jr., P. Smith, T. Smith, R. T. Snider, R. D. Stambaugh, R. Stav, H. St. John, R. E. Stockdale, E. J. Strait, R. Street, T. S. Taylor, J. Tooker, M. Tupper, S. K. Wong, and S. Yamaguchi, Plasma Phys. and Contr. Nucl. Fusion Research 1986 (International Atomic Energy Agency, Vienna, 1987) Vol. I, p. 159.

[13]K. H. Burrell, S. L. Allen, G. Bramson, N. H. Brooks, R. W. Callis, T. N. Carlstrom, M. S. Chu, A. P. Colleraine, D. Content, J. C. DeBoo, R. R. Dominguez, J. R. Ferron, R. L. Freeman, P. Gohil, C. M. Greenfield, R. J. Groebner, G. Haas, W. W. Heidbrink, D. N. Hill, F. L. Hinton, R.-M. Hong, W. Howl, C. L. Hsieh, G. L. Jackson, G. L. Jahns, R. A. James, A. G. Kellman, J. Kim, L. L. Lao, E. A. Lazarus, T. Lehecka, J. Lister, J. Lohr, T. C. Luce, J. L. Luxon, M. A. Mahdavi, H. Matsumoto, M. Mayberry, C. P. Moeller, Y. Neyatani, T.Ohkawa, N. Ohyabu, T. Okazaki, T. H. Osborne, D. O. Overskei, T. Ozeki, A. Peebles, S. Perkins, M. Perry, P. I. Petersen, T. W. Petrie, R.Philipona, J. C. Phillips, R. I. Pinsker, P. A. Politzer, R. P. Seraydarian, M. Shimada, T. C. Simonen, R. T. Snider, G. M. Staebler, B. W. Stallard, R. D. Stambaugh, R. D. Stav, H. St. John, R. E. Stockdale, E. J. Strait, P. L. Taylor, T. S. Taylor, P. K. Trost, U. Stroth, R. E. Waltz, S. M. Wolfe, R. W. Wood, D. Wroblewski, Plasma Phys. and Controlled Fusion **31**, 1649 (1989).

[14]T. N. Carlstrom, P. Gohil, J. G. Watkins, K. H. Burrell, S. Coda, E. J. Doyle, R. J. Groebner, J. Kim, R. A. Moyer, C. L. Rettig, Plasma Phys. and Controlled Fusion **36**, A147 (1994).

[15]R. J. La Haye and J. T. Scoville, in *Proceedings of the 22nd European Physical Society Conference on Controlled Fusion and Plasma Physics,* Bournemonth, 1995, (European Physical Society, Petit-Lancy, 1995) Vol. 19C, Part IV, p. 53.

[16]D. R. Baker, R. T. Snider, M. Nagami, Nucl. Fusion **22**, 807 (1982).

[17]B. Lipshultz, B. LamBombard, E. S. Marmar, M. M.Pickrell, J. L. Terry, R. Watterson, S. M. Wolfe, Nucl. Fusion **24**, 977 (1984).

[18]A. W. Leonard, W. H. Meyer, B. Greer, D. M. Behne, D. N. Hill, Rev. Sci. Instrum. **66**, 1201 (1995)

[19]K. Tsuchiya, H. Takenaga, T. Fukuda, Y. Kamada, S. Ishida, M. Sato, T. Takizuka, and JT-60 Team, in *Proceedings of the 5th Workshop on H–Mode Physics*, Princeton, 1995, to be published in Plasma Phys. and Contr. Fusion.

[20]T. N. Carlstrom, G. L. Campbell, J. C. DeBoo, R. Evanko, J. Evans, C. M. Greenfield, J. Haskovec, C. L. Hsieh, E. McKee, R. T. Snider, R. E. Stockdale, P. K. Trost, M. P. Thomas, Rev. Sci. Instrum. **63**, 4901 (1992)

[21]P. Gohil, K. H. Burrell, R. J. Groebner, J. Kim, W. C. Martin, E. L. McKee, R. P. Seraydarian, in *Proceedings of the 14th Symposium on Fusion Engineering*, San Diego, 1991, (Institute of Electrical and Electronics Engineers, New York, 1992), Vol. 2, p. 1199.

[22]L. L. Lao, H. St. John, R. D. Stambaugh, A. G. Kellman, W. Pfeiffer, Nucl. Fusion **25**, 1611 (1985).

[23]Y. B. Kim, P. H. Diamond, and R. J. Groebner, Phys. Fluids B **3**, 2050 (1991).

ACKNOWLEDGMENTS

This is a report of work supported by the U.S. Department of Energy under Contract No. DE-AC03-89ER51114. The authors wish to thank the DIII–D operation and neutral beam staff, along with the CER and Thomson scattering groups for providing the unique edge data used in this report. Many useful discussion were had with Drs. K.H. Burrell, J.C. DeBoo, R. Maingi, and G.M. Staebler.